The application of artificial neural network in the prediction of the as-cast impact toughness of spheroidal graphite cast iron

Z. Glavaš[1]*, D. Lisjak[2], F. Unkić[1]

[1] *Faculty of Metallurgy, University of Zagreb, Aleja narodnih heroja 3, 44103 Sisak, Croatia*
[2] *Faculty of Mechanical Engineering and Naval Architecture, University of Zagreb, Ivana Lučića 5, 10002 Zagreb, Croatia*

Received 3 August 2006, received in revised form 6 September 2006, accepted 11 September 2006

Abstract

This paper presents the application of artificial neural network (ANN) in the foundry process. Two-layer feedforward neural network which is trained using backpropagation algorithm that updates weights and biases values according to gradient descent momentum and an adaptive learning rate (Backpropagation Neural Network – BPNN) has been established to predict the as-cast impact toughness of spheroidal graphite cast iron (SGI) using the thermal analysis (TA) parameters as inputs. Generalization property of the developed ANN is very good, which is confirmed by a very good accordance between the predicted and the targeted values of as-cast impact toughness on a new data set that was not included in the training data set.

Key words: spheroidal graphite cast iron, impact toughness, artificial neural networks, thermal analysis

1. Introduction

Spheroidal graphite cast iron (SGI), also known as ductile cast iron and nodular cast iron, is a kind of cast iron whose most important microstructural feature is the presence of graphite nodules in the metal matrix. It is a specific engineering material, which possesses good mechanical properties, castability, machinability, and particularly important, it has low production costs. Due to favorable combination of mechanical properties (high tensile strength and good ductility), SGI is used in many applications, such as pipes, various automotive parts etc.

The mechanical properties of SGI are determined by the chemical composition, microstructural properties and conditions during the solidification and the afterwards cooling [1–8]. The microstructure of SGI is determined in part during the solidification and in part during the following eutectoid (solid state) transformation. The shape of graphite is established during the solidification and it cannot be changed afterwards. In the as-cast condition, the typical metal matrix of SGI consists of ferrite and pearlite.

The most important factors which influence the impact toughness of SGI are: chemical composition, the shape and distribution of graphite, nodule count, the cooling rate during the solidification, the cooling rate through the eutectoid transformation range (solid state transformations) and the presence of other microstructural constituents (for example: carbides, iron phosphide etc.).

Chemical composition is one of the most significant factors in determining the metal matrix structure [1, 4–6]. The impact toughness of SGI depends strongly on the ferrite contents in the metal matrix. The SGI with ferritic metal matrix has lower tensile strength, but higher impact toughness and elongation. Si is a ferrite promoter, while elements such as Cu, Sn, Sb, Mn, Cr etc. are pearlite promoters. With the goal of producing as-cast ferritic SGI, the contents of pearlite promoters and carbides promoters (Cr, Mn, etc.) should be kept as low as possible. P is a very harmful element because it has a strong embrittling effect and should be kept as low as possible.

Graphite nodularity has a significant influence on the impact toughness of SGI. Low graphite nodular-

*Corresponding author: tel./fax: +385 44 5333 78; e-mail address: glavaszo@siscia.simet.hr

ity and the presence of non-spheroidal graphite forms result in low values of the impact toughness. Nodule count affects the ferrite/pearlite ratio. As nodule count increases, the diffusional paths of carbon in the eutectoid transformation range decrease, which results in higher ferrite volume fraction in the microstructure for the same chemical composition and cooling conditions [2, 5, 7, 8]. Inoculation has an important influence on graphite nodularity and nodule count. Proper inoculation will improve the nucleation state of the melt, which results in higher nodule count and graphite nodularity.

The effects of the cooling rate on the microstructure and the impact toughness of SGI are quite complex, since they affect both graphite morphology and the ferrite/pearlite ratio. Higher cooling rates during the solidification will increase graphite nodule count and graphite nodularity. However, higher cooling rates in the eutectoid transformations range result in higher volume fraction of pearlite in the microstructure [2, 5, 7, 8].

It is obvious that there is a large number of factors which influence the as-cast impact toughness of SGI. The chemical composition of the cast iron melt does not give the insight into the quality and the predisposition of the base melt in order to obtain sound castings of the required microstructural and mechanical properties (for example as-cast impact toughness). The melt control method, which gives the insight into the metallurgical state of the melt, is thermal analysis (TA). Thermal analysis is a simple, quick and reliable method for the estimation of melt quality and observation of solidification process of cast irons. In the foundries, thermal analysis is performed by recording of cooling curves. The cooling curve is a plot of the temperature as a function of time for a melt sample poured into a standardized cup with thermocouple (Quik-cup®). The parameters, which are identified and measured by thermal analysis, could be applied in the estimation of influence of process parameters on solidification, i.e. for the estimation of metallurgical state of the melt. Many attempts have been made to correlate the data from the cooling curve with the shape of graphite, microstructural and mechanical properties in order to obtain a reliable system for melt control [7–13]. In this paper thermal analysis is used for the estimation of metallurgical state of the melt and the observation of solidification process. The data from the cooling curves are correlated with the as-cast impact toughness of SGI.

The models for the prediction of cast iron properties based on multiple linear regression technique could be applied, more or less successfully, only to specific process conditions under which they have arised. Meanwhile, casting production process is a complicated and nonlinear process, i.e. chemical composition, metallurgical state of the melt and casting properties are not in linear relationship. In recent years, rapid progress in artificial intelligence enables us to use a new method for information processing – artificial neural networks (ANN) [14–17]. ANN are complex systems composed of simple elements (artificial neurons) operating in parallel. These elements (neurons), inspired by biological nervous systems, are in a specific interaction, mutually and with the environment of the system (weights of artificial neural networks), so that they build a functional unit. Two or more neurons may be combined in a layer, and a particular network might contain one or more layers (input layer, output layer and some hidden layers). The number of inputs to the network is designated by the problem, and the number of neurons in the output layer is designated by the number of outputs required by the problem. However, the designer has to define the number of layers between the network input and the output layer and the size of the layers (number of neurons).

The network function is determined by the connections between elements. We can train (learn) ANN to perform a particular function by adjusting the values of the connections (weights) between elements. Each input to neuron is weighted with an appropriate weight. The sum of the weighted inputs and the bias forms the input to the neuron transfer function. It is the function that maps a neuron's (or layer's) net output to its actual output. The most popular transfer functions are linear, log sigmoid, hyperbolic tangent sigmoid etc. The bias is much like the weight, except that it has a constant input of 1.

Properly trained ANN are capable to map input to output patterns with minimal error between the modelled and the measured output values. Testing of ANN follows after training. It is performed by a new input data set, which is not included in the input data set for training of ANN.

Currently, the most important and the most widely used algorithm for neural network training (learning) is backpropagation. This algorithm uses mean squared error and gradient descent for training.

In this paper, Backpropagation neural network (BPNN) was used to predict the as-cast impact toughness of SGI using the TA parameters as inputs.

2. Experimental

In this paper, examinations were performed in the commercial foundry in real industrial conditions. The base melt for the production of SGI was produced in an acid-lined cupola furnace (diameter 800 mm, cold air, capacity 4–5 t/h). The charge materials consisted of special low-manganese pig iron, returns scrap and steel scrap. The melt was transferred to the net-frequent induction furnace, capacity 4 t and power 1110 kW, where its temperature was

Table 1. Average chemical composition (wt.%) of the SGI melts used in the experiments

C	Si	Mn	P	S	Ni	Cr
3.6–3.8	2.7–3.2	0.2–0.3	0.030–0.045	0.001–0.010	0.04–0.06	0.05–0.07
Cu	Mo	Ti	Al	Sn	Mg	
0.07–0.12	0.004–0.011	0.014–0.025	0.009–0.017	0.005–0.015	0.029–0.034	

raised due to the homogenization and correction of chemical composition. After that, the melt was desulphurized in a 3 t ladle by the addition of CaC_2 and strongly mixed with inert gas (nitrogen), which was introduced through a porous plug located at the ladle bottom. After desulphurization and removing of slag the melt was poured into a channel-type induction holding furnace (receptor), capacity 20 t and power 800 kW. The nodularizing treatment of the base melt was performed by Flotret or Osmose method via FeSiMg5 alloy. After the treatment, the sample of melt was taken for thermal analysis and the estimation of chemical composition and a Y-block was cast. Chemical composition of the tested SGI samples was determined with a LECO GDS-400A spectrometer.

Thermal analysis was performed by the advanced thermal analysis system ATAS® (Adaptive Thermal Analysis System). A sample of the melt was poured into a standardized mould with a thermocouple (Quik-cup®). The Y-block was cast in the mould, had been produced by the Betaset process. The dimensions and the form of the Y-block are specified according to the EN 1563. Altogether, 139 melts have been made.

Standard test pieces with V-notch for the estimation of as-cast impact toughness were machined from Y-blocks. The dimensions and the form of the test pieces are specified according to the EN 10045-1 (length of test piece is 55 mm; square section with 10 mm sides; V-notch of 45°, 2 mm deep with a 0.25 mm radius of curvature at the base notch). Test pieces have always been taken from the same place in the Y-block. Altogether, 267 standard test pieces have been made and tested, i.e. 267 input/output pairs of data were available for modelling by ANN.

The impact energy is measure of as-cast impact toughness. The impact energy of SGI samples in as-cast condition was examined by the Charpy method at 20 °C according to EN 10045-1. In this examination a testing machine with maximum striking energy of 15 J was applied.

Metallographic examinations were performed after Charpy impact test by a light metallographic microscope with a digital camera and the image analysis system (AnalySIS® Materials Research Lab).

The goal of these examinations was to establish a neural network model for predicting of the as-cast impact toughness of SGI using data from cooling curves as inputs.

3. Results

3.1. Chemical composition

Average chemical composition of examined SGI melts is given in Table 1.

Deviations from the chemical composition given in Table 1 were present on few melts. High content of P was present on melts number 52–55 (0.067–0.072 %) and melts number 87–92 (0.085–0.11 %). In melts number 43 and 69 high content of Cu (0.57 % and 0.40 %, respectively) was present, while on melts number 135 and 136 high content of Cr (0.26 % and 0.30 %, respectively) was present. These melts of SGI have achieved low values of as-cast impact toughness. The mentioned elements have influence on equilibrium and transformation temperatures, which was reflected on the cooling curves. The analysis of the cooling curves in the eutectoid range shows that high content of Cu influences the decrease of eutectoid transformation temperature, while high content of P influences the increase of eutectoid transformation temperature.

3.2. ANN architecture

The selection of the input parameters is a very important step in ANN modelling. It is based on the physical background of the process. It is very important to select and include all relevant input parameters.

The input parameters for the ANN were thermal parameters derived from the cooling curve in the eutectic and the eutectoid range and thermal parameters derived from first derivative of the cooling curve in the eutectic range. Only those thermal parameters, which have the most important influence on the impact toughness of SGI, were selected as input parameters of the ANN. They are:

– ϑ_{L} – liquidus temperature (°C),

– $\vartheta_{\mathrm{Elow}}$ – the lowest eutectic temperature or temperature of eutectic undercooling (°C),

– ϑ_{R} – recalescence (°C),

– ϑ_{S} – solidus temperature (°C),

– GRF1 (Graphite Factor 1) – a parameter that is defined as the relative time for the temperature to drop 15 °C from the highest eutectic temperature $\vartheta_{\mathrm{high}}$,

– GRF2 (Graphite Factor 2) – a parameter that is calculated from the cooling rate before and after

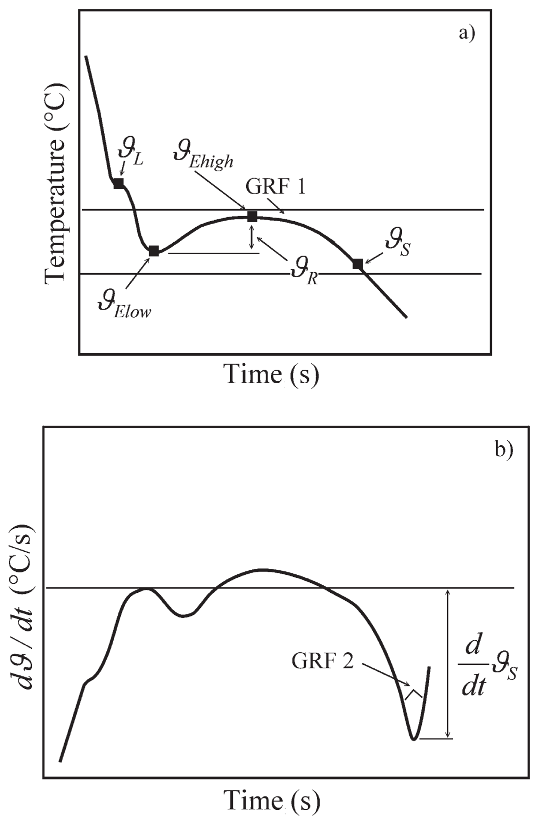

Fig. 1. a) Schematic description of the cooling curve of the SGI in the eutectic range with displayed TA parameters, b) schematic description of the first derivative of the cooling curve in the eutectic range with displayed TA parameters.

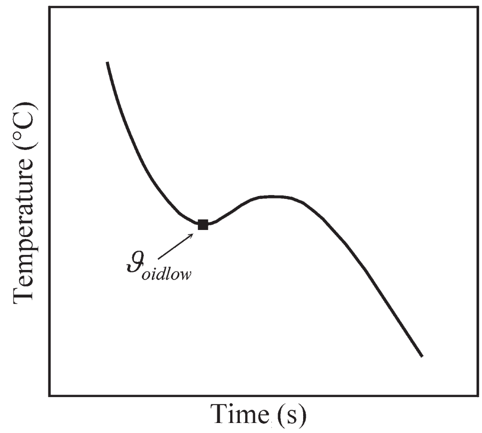

Fig. 2. Schematic description of the cooling curve of the SGI in the eutectoid range with displayed TA parameter.

solidus. The angle of the first derivative at the solidus temperature ϑ_S and the negative peak at the latest segment of the first derivative are used to calculate GRF2,

– $\frac{\mathrm{d}}{\mathrm{d}t}\vartheta_S$ – value of the first derivative at solidus temperature or the depth of the first derivative (negative peak) at solidus (℃/s),

– ϑ_{oidlow} – low eutectoid temperature (℃).

Figures 1a,b and 2 schematically show the selected input parameters of the ANN on the cooling curve in the eutectic range, on the first derivative of the cooling curve in the eutectic range and on the cooling curve in the eutectoid range, respectively.

The software used to create the ANN which predicts the as-cast impact toughness of SGI using the selected TA parameters is Neural Network Toolbox of MATLAB® 7.0.

The network generalization is good when a network is able to perform as well on a test set as on a training set. In this work the generalizability of the network (prevention of overfitting) was performed by the early stopping method. Experimental data set is divided into three subsets: training set (50 % of the experimental data), validation set (25 % of experimental data) and test set (25 % of experimental data). Training set is used for computing the gradient and updating the network weights and biases. Training was performed only on the training set. Validation set was not included in training set and was used to decide when to stop the training. The error on the validation set is monitored during the training process. The validation error will normally decrease during the initial phase of training, as does the training set error. However, when the network begins to overfit the data, the error on the validation set will typically begin to rise. When the validation error increases in a specified number of iterations, the training is stopped, and the weights and biases are returned at the minimum of the validation error. The test set error was not used during the training, but it was used for comparison of different models. To produce the most efficient training, the input and output data are normalized before training.

In this paper different network architectures were examined to determine the network, which has a minimum generalization error. Optimum structure of network (number of layers, number of neurons, transfer functions, learning rate, momentum) was obtained using genetic algorithms (GA). When an optimum network is found, the entire data was used to adjust the weights and biases without changing the structure of the network.

The best results were achieved by a multilayer feedforward neural network which was trained using backpropagation algorithm that updates weights and biases values according to gradient descent momentum and an adaptive learning rate (Backpropagation Neural Network – BPNN). The architecture and parameters of the selected network (BPNN) are given in Table 2.

Table 2. Architecture and parameters of the selected neural network (BPNN)

Number of hidden layers	2
Number of neurons in the first hidden layer	10
Number of neurons in the second hidden layer	9
Number of neurons in the output layer	1
Transfer function of the first hidden layer	Linear transfer function ('purelin')
Transfer function of the second hidden layer	Hyperbolic tangent sigmoid transfer function ('tansig')
Transfer function of the output layer	Linear transfer function ('purelin')
Learning rate	0.451055
Ratio to increase learning rate	1.05
Ratio to decrease learning rate	0.70
Maximum performance increase	1.04
Momentum	0.459628

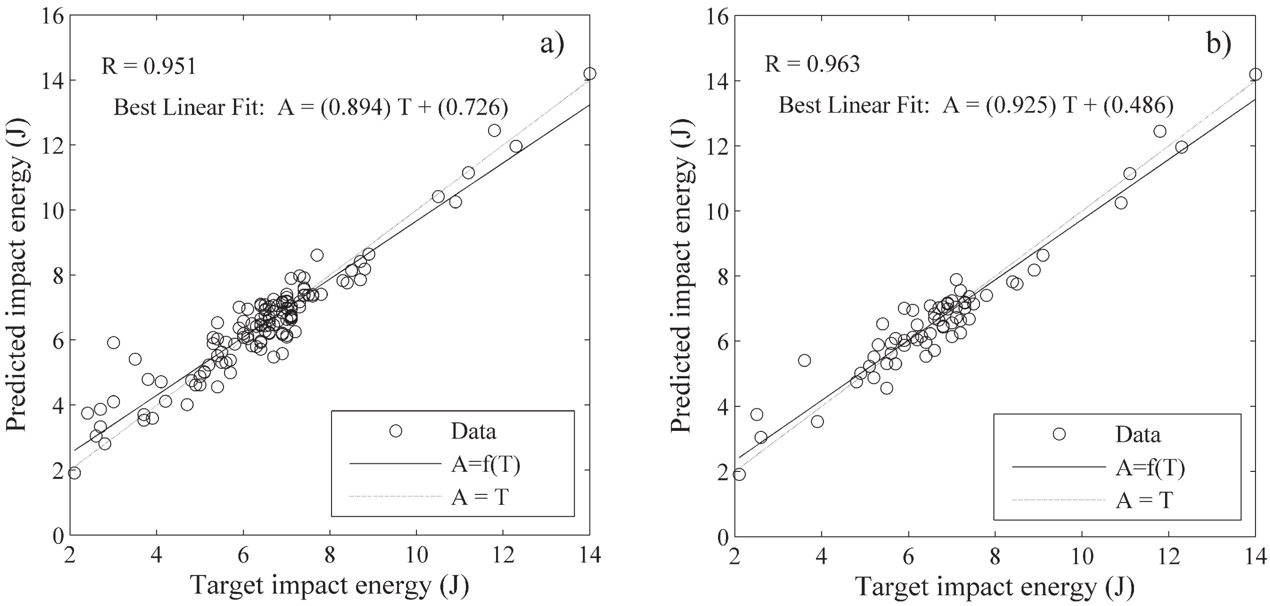

Fig. 3. a) Performance of the BPNN on the training data set, b) performance of the BPNN on the validation data set, R – coefficient correlation, A – predicted impact energy, T – target impact energy.

3.3. Analysis of ANN performance

The performance of a trained BPNN was measured by regression analysis between the network outputs and the corresponding target values, had been obtained by measuring. Figures 3a,b show the performance of the BPNN on the training and validation data set.

The performance functions are important measures for the evaluation of network's performance. In this paper, the performance functions used for training BPNN are the Sum Square Error (SSE), the Mean Square Error (MSE), the Root Mean Square Error (RMSE) and the Normalized Root Mean Square Error (NRMSE). Values of the performance functions on training and validation data set are given in Table 3.

Figures 3a,b show that BPNN very well represents training and validation data set, which is confirmed by high values of coefficient correlations between the network outputs and the corresponding target values obtained by measuring.

High correlation between the network outputs and target values, obtained on training data set, is not a guarantee that network is learned to generalize to new situations.

Therefore, the performance of the BPNN on the test data set was evaluated. The test data set was not used during the training. The performance of the BPNN on the test data set was also measured by regression analysis between the network outputs and the corresponding targets values had been obtained by measuring as well as by the network's performance functions (SSE, MSE, RMSE, NRMSE) (Table 3).

Figure 4a shows a very good network generalization, which is the indication of proper network architecture and proper selection of input network parameters. Figure 4b shows the performance of the BPNN on the entire data set.

T a b l e 3. Values of performance functions on training, validation and test data set

Data set	Performance function			
	SSE	MSE	RMSE	NRMSE
Training set	45.4009	0.3388	0.5821	0.3101
Validation set	19.8724	0.3011	0.5487	0.2685
Test set	29.5433	0.4409	0.6640	0.3628

T a b l e 4. Comparison of target and predicted impact energy (as-cast impact toughness) of SGI (part of test data set)

Network inputs (TA parameters)								Impact energy (J)	
ϑ_{L} (°C)	$\vartheta_{\mathrm{Elow}}$ (°C)	ϑ_{R} (°C)	ϑ_{S} (°C)	GRF1	GRF2	$\frac{\mathrm{d}}{\mathrm{d}t}\vartheta_{\mathrm{S}}$ (°C/s)	$\vartheta_{\mathrm{oidlow}}$ (°C)	Measured	Predicted by BPNN
1139.1	1139.2	4.9	1096.8	90	65	–2.71	734.9	6.0	6.09
1139.5	1139.5	8.5	1095.9	70	61	–2.91	733.9	6.2	7.10
1145.9	1146.0	2.8	1104.9	95	74	–2.59	733.4	5.9	5.87
1143.3	1143.3	5.9	1100.6	88	70	–2.73	733.7	6.5	6.23
1149.2	1149.2	2.8	1103.7	95	35	–3.50	735.9	11.2	11.15
1147.1	1147.1	2.5	1100.3	97	72	–2.68	739.6	6.0	6.20
1148.8	1148.8	4.0	1106.6	91	29	–3.62	737.9	14.0	14.20
1139.7	1139.8	6.7	1097.4	88	54	–3.02	736.2	7.2	7.18
1136.7	1136.6	4.9	1094.9	80	53	–3.02	733.5	7.0	7.41
1136.7	1136.7	5.7	1093.8	81	45	–3.23	736.0	8.8	8.42
1137.8	1137.8	3.6	1092.5	79	50	–3.00	738.9	7.0	6.98
1142.1	1142.1	1.0	1095.8	93	41	–3.38	737.8	10.5	10.41
1139.1	1139.5	6.2	1093.8	87	46	–3.30	746.0	3.6	5.41
1143.2	1143.2	3.9	1099.7	97	80	–2.45	745.3	3.8	3.70
1137.3	1137.5	8.2	1092.6	73	53	–3.15	739.7	7.5	7.38
1146.3	1146.3	6.2	1105.3	86	77	–2.56	739.2	5.4	6.03
1139.6	1139.6	7.9	1097.1	82	58	–2.88	736.6	6.6	7.09
1143.6	1143.6	2.4	1094.3	69	53	–2.99	730.5	2.7	3.87
1139.9	1139.9	2.3	1094.5	70	48	–3.10	733.8	7.1	7.17
1142.5	1142.5	1.7	1094.3	88	48	–3.14	736.3	7.5	7.36
1140.6	1140.5	7.1	1099.8	78	64	–2.80	734.4	6.5	5.92
1137.3	1137.5	8.1	1092.2	65	117	–2.18	746.7	2.8	2.81
1143.0	1143.0	0.7	1095.8	76	44	–3.22	741.3	7.3	7.97
1142.2	1142.2	9.4	1103.6	77	47	–3.14	733.5	3.0	5.92
1138.6	1138.6	6.6	1094.1	76	61	–2.84	741.7	6.2	6.11
1141.5	1141.5	7.1	1096.7	79	61	–2.89	743.5	6.5	5.48
1140.8	1140.8	6.5	1097.0	68	52	–2.98	739.1	7.1	6.76
1137.0	1137.0	5.1	1093.7	84	49	–3.08	740.2	7.3	7.17
1144.9	1145.0	2.5	1097.7	94	44	–3.19	740.9	8.5	8.14
1139.5	1139.5	4.9	1093.5	73	48	–3.15	735.5	7.4	7.40

A part of test data set (network inputs and the corresponding target values obtained by measuring) and network outputs are given in Table 4.

4. Discussion

The results of neural network modelling of as-cast impact toughness of SGI based on the data from the cooling curves show that the combination of thermal analysis and neural networks is a powerful tool for the estimation of melt quality, i.e. mechanical properties. A very high correlation coefficient between the measured and the estimated values of impact energy, i.e. as-cast impact toughness on test data set presents successfulness of the model.

Thermal parameters, which were taken as input variables for the neural network, are closely connected with chemical composition and microstructure development of SGI. In the succession of discussion there will be considered the influence of the selected TA parameters on the as-cast impact toughness of SGI.

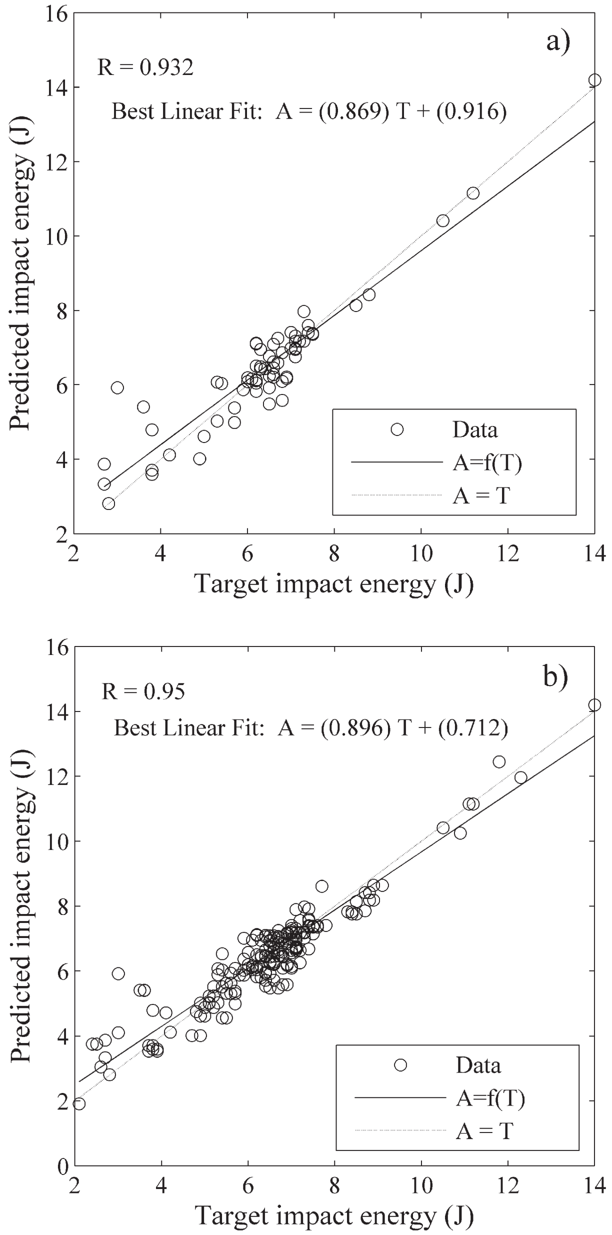

Fig. 4. a) Performance of the BPNN on the test data set, b) performance of the BPNN on the entire data set, R – coefficient correlation, A – predicted impact energy, T – target impact energy.

The liquidus temperature ϑ_{L} (Fig. 1a) is related to the carbon equivalent (CE), i.e. with C and Si contents. Low values of liquidus temperature are primarily the indication of high C contents. Combination of high C contents, i.e. carbon equivalent and slow cooling rates (thick sections) results in flotation and formation of non-spheroidal graphite forms, which has a negative influence on mechanical properties of SGI. Increasing of C contents may result in increasing of nodules count per unit volume and decreasing of the average distance between them [18]. A too high nodules count is not desirable since the graphite nodules may act as voids under a tensile load condition. Decreasing of average distance between graphite nodules (high nodules count) may influence the connection of the voids (graphite nodules) at an earlier stage of the deformation of the metal matrix, which results in decreasing of impact toughness. Although it promotes ferrite, very high Si contents are not favorable since Si strengthens the ferrite, which has a negative influence on the impact toughness of SGI [3, 19].

Liquidus temperature ϑ_{L}, the temperature of the start of eutectic reaction ϑ_{ES} and the lowest eutectic temperature $\vartheta_{\mathrm{Elow}}$ of the examined melts are almost the same temperatures, which indicates equal precipitation of eutectic during the solidification, i.e. continuous nucleation of graphite. Continuous nucleation of graphite during the solidification results in high density of graphite particles in the metal matrix. During the eutectoid transformation, i.e. austenite decomposition, high density of graphite particles (a higher number but not very high) acts on decreasing of diffusional paths of C in the solid state, which results in increasing of the fraction of ferrite in the microstructure. The increase of amount of ferrite in the metal matrix of SGI results in increasing of the impact toughness.

The lowest eutectic temperature or temperature of eutectic undercooling $\vartheta_{\mathrm{Elow}}$ (Fig. 1a) is related to the nucleation state of the melt. Low value of temperature of eutectic undercooling indicates poor nucleation properties of the melt, i.e. a low number of active sites for nucleation of graphite. Moreover, if the temperature of eutectic undercooling lies below the metastable temperature, primary carbides may accrue in the microstructure. Low density of graphite particles, i.e. graphite nodules in the metal matrix and the presence of carbides in the microstructure, has a negative influence on impact toughness of SGI.

Recalescence ϑ_{R} (Fig. 1a) represents the difference between the highest eutectic temperature $\vartheta_{\mathrm{high}}$ and the lowest eutectic temperature (temperature of eutectic undercooling) $\vartheta_{\mathrm{Elow}}$. Recalescence is the indicator of the eutectic growth, i.e. the amount of austenite and graphite that are precipitated during the early stage of eutectic solidification. High recalescence indicates the poor nucleation properties of the melt. Moreover, high recalescence is related to the non-continuous precipitation of graphite during the solidification. Too high amount of graphite precipitated in the early stage of eutectic solidification results in a small amount of available graphite during the later solidification. Due to that, secondary sites of nucleation are not activated, which may result in a low nodule count.

Solidus temperature ϑ_{S} (Fig. 1a) is an important thermal parameter for monitoring the end of the solidification. Segregation of carbide forming elements such as Cr, Mn, V etc. at cell boundaries causes an increase of the metastable temperature. If the solidus temperature lies below the metastable temperature, intercellular carbides may accrue in the microstructure. Intercellular carbides have a negative influence on the impact toughness of SGI.

GRF1 (Fig. 1a) is the parameter that reflects how much eutectic, i.e. eutectic graphite is precipitated during the second part of eutectic (from $\vartheta_{\mathrm{high}}$ to ϑ_{S}). A high GRF1 indicates continuous precipitation of eutectic graphite, which is related to the activation of secondary nucleation sites. This results in the moving of the eutectic reaction toward longer times. This mode of eutectic solidification, when the nucleation and the growth of eutectic occur in longer times, results in a higher distribution of sizes of the precipitated graphite, i.e. a higher density of graphite particles in the metal matrix. A higher number of graphite particles during the eutectoid transformation enable the formation of a higher fraction of ferrite in the microstructure, i.e. higher impact toughness.

GRF2 (Fig. 1b) is a parameter that reflects the change of the cooling rate at the end of the solidification, measuring indirectly thermal conductivity. Low value of GRF2 indicates high thermal conductivity, which is an indicator of a high amount of graphite at the end of the solidification. Low value of the first derivative of the cooling curve at solidus (higher depth of the negative peak) $\frac{\mathrm{d}}{\mathrm{d}t}\vartheta_{\mathrm{S}}$ (Fig. 1b) is related to the high amount of eutectic graphite at the end of the solidification, i.e. a high nodule count in the SGI. Therefore, GRF2 combined with $\frac{\mathrm{d}}{\mathrm{d}t}\vartheta_{\mathrm{S}}$ is a strong indicator of thermal conductivity, i.e. the graphite shape and nodule count in SGI.

The eutectoid transformation has an important influence on the final microstructure of SGI. The solid state transformation of austenite into ferrite and pearlite occurs at the eutectoid temperature. The fraction of ferrite and pearlite in the microstructure of SGI depends on the chemical composition, the cooling rate through the eutectoid transformation range, the volume fraction and the number of graphite nodules. When pearlite is created latent heat is released, which is visible as an arrest in the cooling curve. At higher amounts of pearlite, recalescence occurs during the eutectoid transformation. Recalescence represents the difference between the high ($\vartheta_{\mathrm{oidhigh}}$) and the low eutectoid temperature ($\vartheta_{\mathrm{oidlow}}$). The place of the low eutectoid temperature ($\vartheta_{\mathrm{oidlow}}$) on the cooling curve in the eutectoid range is presented on Fig. 2. A fully ferritic SGI does not show recalescence. It has also been found that the increasing of the amounts of pearlite in the metal matrix lowers the low eutectoid temperature. Therefore, the low eutectoid temperature is the indicator of the fraction of pearlite in the metal matrix of SGI. The impact toughness of SGI decreases with the increase of the amount of pearlite in the metal matrix.

5. Conclusions

Artificial neural networks (ANN) are a powerful tool which enables the engineer to study and analyse complex interactions between the material and process inputs with the goal of predicting final component properties. Developed Backpropagation Neural Network (BPNN) successfully predicts the as-cast impact toughness of SGI using the TA parameters as inputs. A very good accordance between the measured and the predicted as-cast impact toughness was achieved.

The obtained results show that the analysis of the cooling curve and neural network modelling enables the formation of mathematical models for the prediction of microstructural and mechanical properties of cast irons before pouring of the melt into the moulds. This allows for corrective measures to be taken with the purpose of obtaining the required microstructural and mechanical properties of castings as well as the decrease in the percentage of the waste castings.

References

[1] VENUGOPALAN, D.: Metallurgical Transactions A, *21*, 1990, p. 913.
[2] GUO, X.—STEFANESCU, D. M.: AFS Transactions, *105*, 1997, p. 533.
[3] PAN, E. N.—HSU, W. S.—LOPER, C. R.: AFS Transactions, *96*, 1988, p. 645.
[4] VENUGOPALAN, D.: AFS Transactions, *98*, 1990, p. 465.
[5] SKALAND, T.—GRONG, Ø.: AFS Transactions, *99*, 1991, p. 153.
[6] VENUGOPALAN, D.—ALAGARSAMY, A.: In: Proceedings of the Fourth International Symposium on the Physical Metallurgy of Cast Iron. Eds.: Ohira, G., Kusakawa, T., Niyama, E. Tokyo, Materials Research Society 1989, p. 321.
[7] MRVAR, P.: Scandinavian Journal of Metallurgy, *31*, 2002, p. 393.
[8] MRVAR, P.: Materials Science Forum, *508*, 2006, p. 287.
[9] STEFANESCU, D. M.: In: Proceedings of the Third International Symposium on the Physical Metallurgy of Cast Iron. Eds.: Fredriksson, H., Hillert, M. Stockholm, Materials Research Society 1984, p. 151.
[10] LABRECQUE, C.—GAGNÉ, M.: AFS Transactions, *106*, 1998, p. 83.
[11] CHANG, S.—SHANGGUAN, D.—STEFANESCU, D. M.: AFS Transactions, *99*, 1991, p. 531.
[12] BHASKARAN, C. A.—WIRTH, D. J.: AFS Transactions, *110*, 2002, CD-ROM issue, paper 02–003.
[13] GLAVAŠ, Z.—UNKIĆ, F.—MAJSTOROVIĆ, Š.: Strojarstvo, *47*, 2005, p. 77.

[14] HAGAN, M. T.—DEMUTH, H. B.—BEALE, M. H.: Neural Network Design. Boston, PWS Publishing Company 1996.
[15] YAO, R. B.—TANG, C. X.—SUN, G. X.: AFS Transactions, *104*, 1996, p. 635.
[16] XU, J. L.—WANG, Z. P.—CHEN, C.: AFS Transactions, *110*, 2002, CD-ROM issue, paper 02–013.
[17] DJURDJEVIĆ, M. B.—FRANCIS, R.—LASHKARI, R. S.—NGOM, A.—SOKOLOWSKI, J. H.: AFS Transactions, *111*, 2003, CD-ROM issue, paper 03–095.
[18] KOMATSU, S.—SHIOTA, T.—NAKAMURA, K.: In: Proceedings of the Fourth International Symposium on the Physical Metallurgy of Cast Iron. Eds.: Ohira, G., Kusakawa, T., Niyama, E. Tokyo, Materials Research Society 1989, p. 313.
[19] UNKIĆ, F.—GAVRANOVIĆ, N.—VASILIĆ, M.: Strojarstvo, *47*, 2005, p. 33.